Chemotactic Activity of S100A7 (Psoriasin) Is Mediated by the Receptor for Advanced Glycation End Products and Potentiates Inflammation with Highly Homologous but Functionally Distinct S100A15[1]

Ronald Wolf,* O. M. Zack Howard,§ Hui-Fang Dong,¶ Christopher Voscopoulos,* Karen Boeshans,‖ Jason Winston,* Rao Divi,* Michele Gunsior,‡ Paul Goldsmith,‡ Bijan Ahvazi,‖ Triantafyllos Chavakis,† Joost J. Oppenheim,§ and Stuart H. Yuspa[2]*

Human S100A7 (psoriasin) is overexpressed in inflammatory diseases. The recently discovered, co-evolved hS100A15 is almost identical in sequence and up-regulated with hS100A7 during cutaneous inflammation. The functional role of these closely related proteins for inflammation remains undefined. By generating specific Abs, we demonstrate that hS100A7 and hS100A15 proteins are differentially expressed by specific cell types in the skin. Although highly homologous, both proteins are chemoattractants with distinct chemotactic activity for leukocyte subsets. We define RAGE (receptor for advanced glycation end products) as the hS100A7 receptor, whereas hS100A15 functions through a Gi protein-coupled receptor. hS100A7-RAGE binding, signaling, and chemotaxis are zinc-dependent in vitro, reflecting the previously reported zinc-mediated changes in the hS100A7 dimer structure. When combined, hS100A7 and hS100A15 potentiate inflammation in vivo. Thus, proinflammatory synergism in disease may be driven by the diverse biology of these almost identical proteins that have just recently evolved. The identified S100A7 interaction with RAGE may provide a novel therapeutic target for inflammation. *The Journal of Immunology,* **2008, 181: 1499–1506.**

Human S100A7 (hS100A7, psoriasin) was first identified as a protein up-regulated in inflamed hyperplastic psoriatic skin (1). Since then, hS100A7 has been widely studied because it is differentially expressed and released during inflammation (2–5). Recently, hS100A15, highly homologous to hS100A7, was also identified as up-regulated in psoriasis, thereby suggesting a role in the inflammatory phenotype (6). However, the characteristics and functional mechanisms that link both hS100A7 and hS100A15 to inflammation are not defined. Both proteins belong to the multigenic S100 family of EF-hand proteins (7, 8). Despite their small size and conserved functional domains, gene duplications and variations throughout vertebrate evolution led to an increase in number and diversity within the S100 family. Genomic analysis of the hS100A7 and hS100A15 encoding chromosomal regions (chromosome 1q21, epidermal differentiation complex) reveals that both evolved recently by gene duplications during primate evolution, diverging the least among all S100 family members (9, 10). Thus, their high homology (93% sequence identity) makes it difficult to distinguish them when co-expressed. To address this further, we have developed unique reagents and functional assays to dissect similarities and differences among these closely related homologs. This study provides insight into properties and functional mechanism of S100A7- and S100A15-induced inflammation and reveals an unexpected biological diversity that may drive their functional synergism in inflammatory diseases.

Materials and Methods

All the materials and methods used have been approved by the National Cancer Institute.

Cloning, protein expression, and purification

cDNA was prepared by PCR cloning of full-length transcripts (hS100A7: NM_002963; hS100A15: AY189119) isolated from human skin 6. Proteins were expressed in *Escherichia coli BL21* (DE3) cells harboring plasmid His^6-myelin basic protein $(MBP)^3$-tev hS100A15/-hS100A7, and proteins were purified as described (11). Purified S100 protein, a single band on Coomassie-stained gels (M_r of ~12 kDa), was purged of endotoxin before experiments by chromatography onto Detoxigel columns (Pierce) with endotoxin levels <0.05 EU/μg protein. Endotoxin levels are below biological activity as demonstrated in vivo and in vitro inflammation and chemotaxis assays demonstrating that neutralization of S100 proteins or heating abrogated functional activity.

Cell culture

Normal human keratinocytes (Cascade Biologics) were cultured in keratinocyte growth medium containing insulin (5 μg/ml) and bovine pituitary

*Laboratory of Cancer Biology and Genetics, †Experimental Immunology Branch, and ‡Antibody and Protein Purification Unit, Center for Cancer Research, National Cancer Institute, Bethesda, MD 20892; §Laboratory of Molecular Immunoregulation, Cancer and Inflammation Program, Center for Cancer Research, and ¶Science Applications International Corp. Frederick, Division of Basic Sciences and Cellular Immunology, National Cancer Institute, Frederick, MD 21702; and ‖X-ray Crystallography Facility, National Institute of Arthritis and Musculoskeletal and Skin Diseases, National Institutes of Health, Bethesda, MD 20892

Received for publication January 14, 2008. Accepted for publication May 17, 2008.

The costs of publication of this article were defrayed in part by the payment of page charges. This article must therefore be hereby marked *advertisement* in accordance with 18 U.S.C. Section 1734 solely to indicate this fact.

[1] R.W. is supported by the German Research Foundation, Emmy-Noether Program (Wo 843/2-1). This work was supported in part by the Intramural Research Program of the National Cancer Institute, Center for Cancer Research, and of the National Institute of Arthritis and Musculoskeletal and Skin Diseases of the National Institutes of Health.

[2] Address correspondence and reprint requests to Dr. Stuart H. Yuspa, Laboratory of Cancer Biology and Genetics, Center for Cancer Research, National Cancer Institute, National Institutes of Health, 37 Convent Drive, MSC-4255, Building 37, Room 4068A, Bethesda, MD 20892. E-mail address: yuspas@mail.nih.gov

[3] Abbreviations used in this paper: MBP, myelin basic protein; CHO, Chinese hamster ovary; GiPCR, Gi protein-coupled receptor; RAGE, receptor for advanced glycation end products.

extract (50 μg/ml) at 37°C in air containing 5% CO_2. Keratinocytes washed twice with PBS were harvested into lysis buffer for protein analysis (Cell Signaling Technology) as described below. Chinese hamster ovary (CHO) cells were cultured in Ham's F12 (Invitrogen) with 10% BSA plus Zeocin (200 μg/ml) for selection of receptor for advanced glycation end products (RAGE) transfectants at 37°C in air containing 5% CO_2 (12).

Establishment of Abs specific for hS100A7 and hS100A15, in vitro stimulation assay, immunoblot analysis, immunofluorescent staining

Monospecific antisera to hS100A15 were prepared in rabbits by injecting a synthetic peptide that corresponds to the N-terminal amino acid sequence of the deduced hS100A15 protein (GenBank accession no. AAO40032). The Abs were affinity purified using the synthetic peptide coupled to Affigel-15 (Bio-Rad). Most of the commercial and donated hS100A7 Abs tested detected both proteins (data not shown). The monoclonal anti-hS100A7 Ab (Imgenex; Abcam) specifically detects recombinant S100A7 monomer without crossreacting with recombinant hS100A15 or several other hS100 proteins (50 ng/lane) (see Fig. 1*A*). hS100A8 and hS100A10 (Novus Biologicals) were used as controls. Additionally, preadsorptions with increasing doses of the corresponding cognate proteins blocked respective S100 Ab staining (Ref. 13 and data not shown).

To measure downstream MAP kinase activity, human granulocytes from normal volunteers were resuspended in RPMI 1640 (Invitrogen) at 10×10^6/ml and were stimulated with 1 μg/ml hS100A7 $\pm$ 15 nM $ZnCl_2$ at 37°C for 5 min before being pelleted followed by removal of media. The pellets were quick frozen in a dry ice/methanol bath. Cells were preincubated with neutralizing anti-RAGE (5 μg/ml, R&D Systems) or soluble RAGE (R&D Systems) 30 min before stimulation.

For immunoblot analysis, total cell lysates of neutrophils, CHO cells, or cultured keratinocytes (20 μg) were prepared using 1% Triton-containing lysis buffer (Cell Signaling Technologies). Proteins were separated using a 12% SDS-polyacrylamide gel, transferred to reinforced nitrocellulose membranes, and visualized by Ponceau stain. Filters were incubated with blocking buffer (TBS (pH 7.4) with 5% milk, 0.1% Tween 20) for 30 min, primary Ab (anti-hS100A15, 1 μg/ml; anti-hS100A7 Ab, 1 μg/ml; anti-phospho-ERK1/2, anti-total ERK1/2, 1:1000, Cell Signaling Technologies; anti-RAGE, 1:250, Santa Cruz Biotechnology; anti-β-actin, 1:20,000, Chemicon International) overnight, and secondary Ab for 1 h with several washes (TBS (pH 7.4), 0.1% Tween 20) between incubations.

Immunoflorescent staining was performed on serial 5-μm frozen sections of human normal and psoriatic skin fixed in acetone. The sections were treated with 96% methanol and 4% H_2O_2, blocked in 10% normal goat serum, and incubated overnight with anti-hS100A15 or anti-hS100A7 (5 μg/ml each). Experiments without primary Abs and serial dilution competition assays were performed in the absence and presence of blocking peptide to determine the optimal working concentration and specificity of the primary hS100A15 Ab. Donkey anti-rabbit Cy3 (1:250) was used as a secondary Ab to the hS100A15 or donkey anti-mouse FITC (1:250) to hS100A7 (The Jackson Laboratory). When sections were co-stained, FITC-labeled Mart-1/Hmb 45 cocktail at 1/25 dilution (monoclonal, Biocare Medical) and MHCII-FITC at 1/250 dilution (Serotec) were mixed with the primary Ab. All sections were nuclear stained with DAPI (Sigma-Aldrich) and mounted. All biopsies were taken with the patient's informed consent and approval of the local ethics committee.

Chemotaxis assays

Human leukocytes from normal volunteers were Percoll purified (95%) from leukopacs provided by the National Institutes of Health blood bank (under IRB 99-CC-0168) as previously described (14). The chemoattractants hS100A7, hS100A15, and CXCL8/IL-8 (PeproTech) were diluted in RPMI 1640 containing 1% BSA and placed in the lower 25 μl chamber. hS100A7 was mixed with $ZnCl_2$ at least 30 min prior to being placed in a chemotaxis chamber. Cells were suspended in the above medium at 0.5–5×10^6/ml and 50 μl was placed in the upper chamber, which was separated from the lower one by a polycarbonate filter (pore size pf 5 μm), which was coated with fibronectin for lymphocyte migration. In selected experiments, neutralizing anti-hRAGE (5 μg/ml), pertussis toxin (50–100 ng/ml), CXCL12 (PeproTech), PD98059 (10 μM), hS100A7, or hS100A15 was added 30 min at 37°C before the cells were added in the upper chamber. Cells were allowed to migrate for 3 h (T lymphocytes), 1 h (granulocytes), or 1.5 h (monocytes) at 37°C in a humidified, 5% CO_2 incubator. Cells attached to the lower filter surface were stained with a rapid stain (Richard-Allan Scientific), counted in six fields, and the averages were expressed as ratio (chemotactic index) of the numbers of cells in the treated sample vs control (spontaneous migration).

In vitro ligand-receptor interactions

Recombinant hS100A7 was biotinylated using *N*-hydroxysuccinimide ester of biotin (NHS-PEO_4-biotin) containing a polyethylene glycol spacer arm that renders/maintains hS100A7 aqueous solubility. hS100A7 (2 mg) dissolved in PBS (0.1 M phosphate, 0.15 M NaCl (pH 7.2)) was mixed with 2 molar excess of NHS-PEO_4-biotin and incubated on ice for 2 h. Biotinylated-S100A7 (biotin-S100A7) was separated from unreacted NHS-PEO_4-biotin using Econo-Pac 10DG column (Bio-Rad) and stored at −80°C until use. Ligand binding assays were performed in 96-well polystyrene plates that were preadsorbed with purified murine recombinant soluble RAGE (100 ng/well) overnight and blocked with 0.25% casein (I-block) (Applied Biosystems). Assays were performed in the presence of the indicated concentration of biotinylated hS100A7 with/without excess of unlabeled recombinant hS100A7, hS100A15, nonimmune IgG (Jackon ImmunoResearch Laboratories), anti-mouse RAGE (R&D Systems), anti-human RAGE (R&D Systems), soluble RAGE (sRAGE; R&D Systems), CXCL8/IL-8, or I-block in PBS (1 mM KH_2PO_4, 3 mM Na_2HPO_4, 155 mM NaCl, 1.2 mM $CaCl_2$, 50 μM $ZnCl_2$) for 90 min at 37°C. Wells were washed rapidly to remove unbound ligand, then incubated with streptavidin alkaline phosphatase (1/1500 dilution) in I-block at room temperature for 60 min, and washed with PBST (PBS containing 0.05% Tween-20), distilled water, and Tris buffer (20 mM Tris, 1 mM $MgCl_2$ (pH 9.5)) before adding CDP-Star containing Emerald II enhancer (Applied Biosystems) and incubating at room temperature for 20 min and at 4°C overnight. Luminescence was measured using a TR717 microplate luminometer (Applied Biosystems). Binding of biotin-S100A7 to RAGE is directly proportional to the amount of luminescence signal in the well and is reported as luminescence units. High-binding polystyrene 96-well plates were obtained from Greiner Bio-One, streptavidin-alkaline phosphatase, I-block (casein), and chemiluminescent substrate (CDP-Star containing Emerald II enhancer) were obtained from Applied Biosystems, and NHS-PEO_4-biotin was from Pierce.

Cell adhesion assays

Control vector or RAGE-transfected CHO cells were allowed to adhere to immobilized hS100A7, hS100A15 (10 μg/ml each), and to BSA (as control) according to a previously described modified protocol (15). Briefly, microtiter plates were coated with the S100 proteins in bicarbonate buffer (pH 9.6) and blocked with 3% BSA solution. Fluorescently labeled (2′,7′-bis-(2-carboxyethyl)-5-(and 6)-carboxyfluorescein acetoxymethyl ester) CHO control or RAGE-vector-transfected cells were washed in serum-free RPMI 1640 medium and plated onto the precoated wells (10^5/well) at 37°C for 60 min in the absence or presence of zinc (50 μM) or neutralizing anti-RAGE or sRAGE (5 μg/ml, R&D Systems). After the 60-min incubation period, the wells were washed and adherent cells were quantified by measuring absorbance at 590 nm.

In vivo peritonitis model

C57BL/6 $RAGE^{-/-}$ mice were characterized previously (15). HBSS (Invitrogen), recombinant native or heat-inactivated S100 proteins (20 μg in 1 ml HBSS/mouse) (16, 17) were administered i.p. into C57BL/6 wild-type and $RAGE^{-/-}$ mice. As control, thioglycollate-induced peritonitis was performed as previously described (12). To evaluate neutrophil recruitment, mice were sacrificed at 4 h after injection. Thereafter, the peritoneal lavage was collected and the numbers of emigrated cells were analyzed by hemocytometry. There was no difference in the circulating neutrophil count of wild-type or $RAGE^{-/-}$ mice. Recovered peritoneal leukocytes were incubated for 5 min with 2.3G2 anti-FcIII/II receptor, then stained at 4°C for 30 min with allophycocyanin-conjugated anti-Gr1 as a neutrophil marker. Cells were fixed with 1% paraformaldehyde, and cytometry was done with a FACSCalibur cytometer (BD Biosciences) and results were analyzed with Diva software (BD Biosciences). Similar results were obtained by analyzing leukocyte populations with conventional smears. All Abs were purchased from BD Pharmingen.

Bioinformatics

The amino acid sequences of the human S100 proteins were aligned using the program T-Coffee (version 2.11).

Statistical analysis

Data were analyzed for statistical significance by ANOVA with post hoc Bonferroni analysis using SPSS (version 15.0), with $p \leq 0.05$ being considered significant.

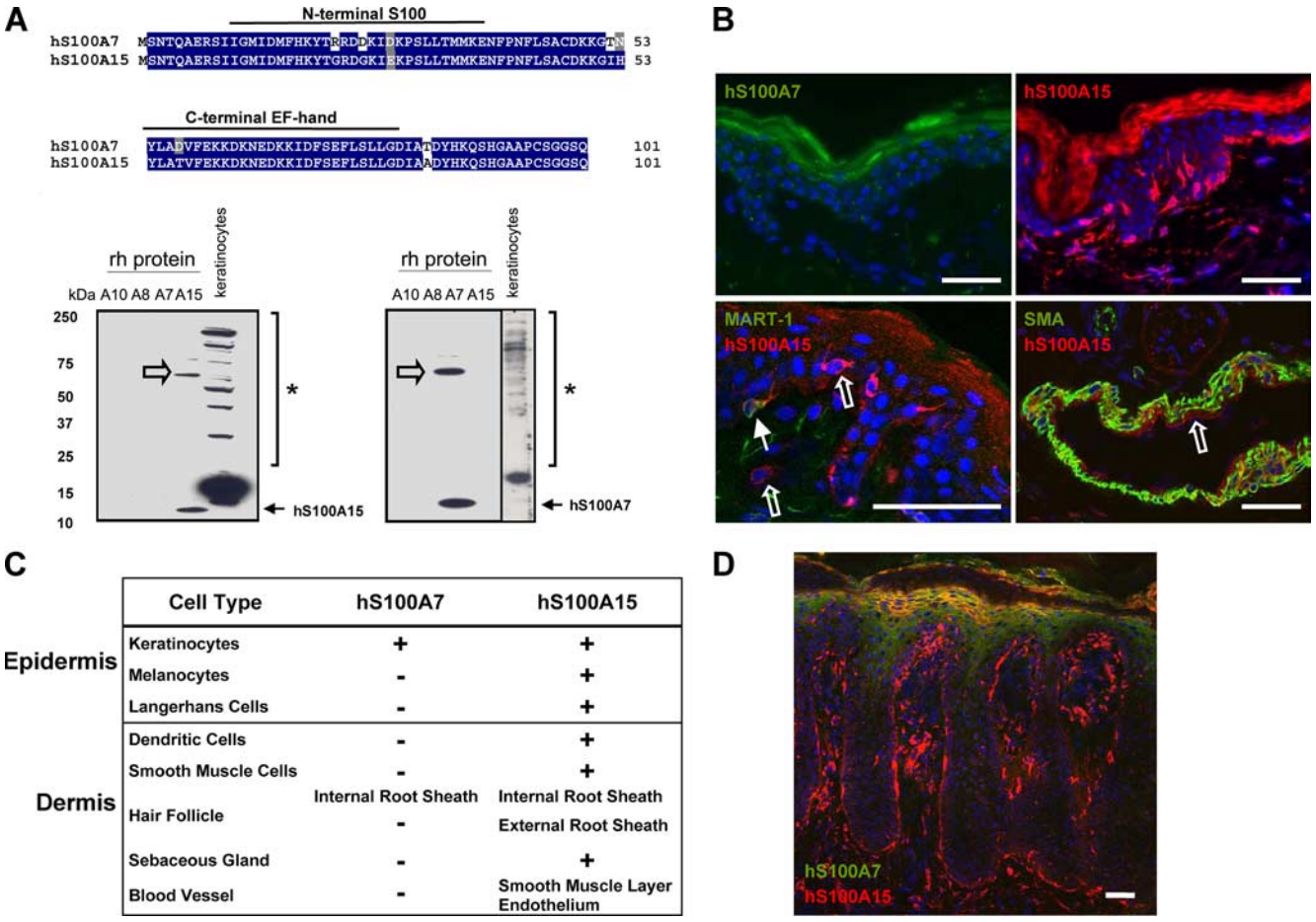

FIGURE 1. Human S100A7 and S100A15 proteins are differentially expressed in human skin. *A*, Alignment of the predicted amino acid sequences of the hS100A7 (NP_002954) with hS100A15 (NP_79669). Identical amino acid residues are indicated as blue boxes, and chemically similar amino acids are marked as gray boxes. Predicted EF-hand motifs for both proteins are marked above the sequences (variant S100-specific motif, aa 12–39; canonical EF-hand, aa 54–82). Indicated recombinant human S100 proteins (50 ng) and human keratinocyte lysates (20 μg), subjected to immunoblotting by incubation with monoclonal anti-hS100A7 or the affinity-purified polyclonal anti-hS100A15 Ab 3923. Solid arrows indicate the migration of the corresponding recombinant hS100A15 and hS100A7 monomers. Both Abs detect the corresponding low- and high-molecular weight forms (asterisks) in keratinocyte lysate. The immunoreactive bands above the recombinant S100 monomers (open arrows) represent uncleaved recombinant MBP-hS100A7 and MBP-hS100A15 fusion proteins. *B*, Immunofluorescent staining of frozen sections of adult human skin stained for hS100A7 (green, *upper left panel*) and hS100A15 Ab (red, *upper right panel*). Co-staining of hS100A15 (red, *lower panels*) with MART-1 (green, *lower left panel*) or smooth muscle actin (green, *lower right panel*). Full arrows indicate melanocytes, hollow arrows Langerhans cells and dendritic cells (*lower left panel*) or vascular endothelial cells (*lower right panel*). Nuclei were stained with DAPI (blue). Bar sizes: 50 μm. *C*, Summary of expression and distribution of hS100A7/A15 in human skin based on immunostaining. *D*, Frozen sections of inflamed lesional psoriasis were stained for hS100A7 (green) and hS100A15 (red). Nuclei were stained with DAPI (blue). Bar size: 50 μm.

Results

hS100A7 and hS100A15 paralogs are differentially expressed

Because hS100A7 and hS100A15 are almost identical in sequence (93%), distinguishing their expression has been difficult (Fig. 1*A*). To address this further, Abs were generated in rabbits to a unique N-terminal sequence in hS100A15. Immunoblotting revealed a single monomer band of recombinant hS100A15 distinct from other S100 proteins and native low- and high-molecular weight bands in keratinocyte lysates, as is typical for many S100 proteins 4 (Fig. 1*A*). The hS100A15 Ab did not detect related recombinant hS100 proteins, particularly hS100A7. Similarly, the monoclonal hS100A7 Ab revealed specific staining of the hS100A7 monomer along with high-molecular weight forms in keratinocyte lysates that were distinct from those detected with the hS100A15 Ab.

Using these specific Abs, the expression and distribution of the corresponding hS100A7 and hS100A15 proteins in human skin were studied. In normal epidermis, hS100A7 expression was confined to the granular/cornified layer only (Fig. 1*B*, *upper left panel*). Human S100A15 colocalized there, but unlike hS100A7, it was expressed by epidermal basal cells and dendritic-shaped cells (Fig. 1*B*, *upper right panel*). By co-staining, these hS100A15-expressing dendritic cells were identified as melanocytes (MART-1 positive), whereas MART-1-negative, hS100A15-positive cells were identified as epidermal Langerhans cells (Fig. 1*B*, *lower left panel*) and dermal dendritic cells (MHCII-positive, not shown). In the dermis, hS100A15 was further expressed by endothelial cells interior to vascular smooth muscle cells (smooth muscle actin-positive) (Fig. 1*B*, *lower right panel*) and other cell types, where hS100A7 and hS100A15 were differentially expressed (summarized in Fig. 1*C*).

Since psoriasis is the prototype of inflammatory disease where hS100A7 and hS100A15 were first identified, our unique hS100A15 Ab provided an opportunity to discriminate the expression of these proteins in psoriatic skin (Fig. 1*D*). Compared with normal skin, both hS100A7 and hS100A15 are up-regulated in inflamed lesional psoriatic skin and co-expressed by the epidermal

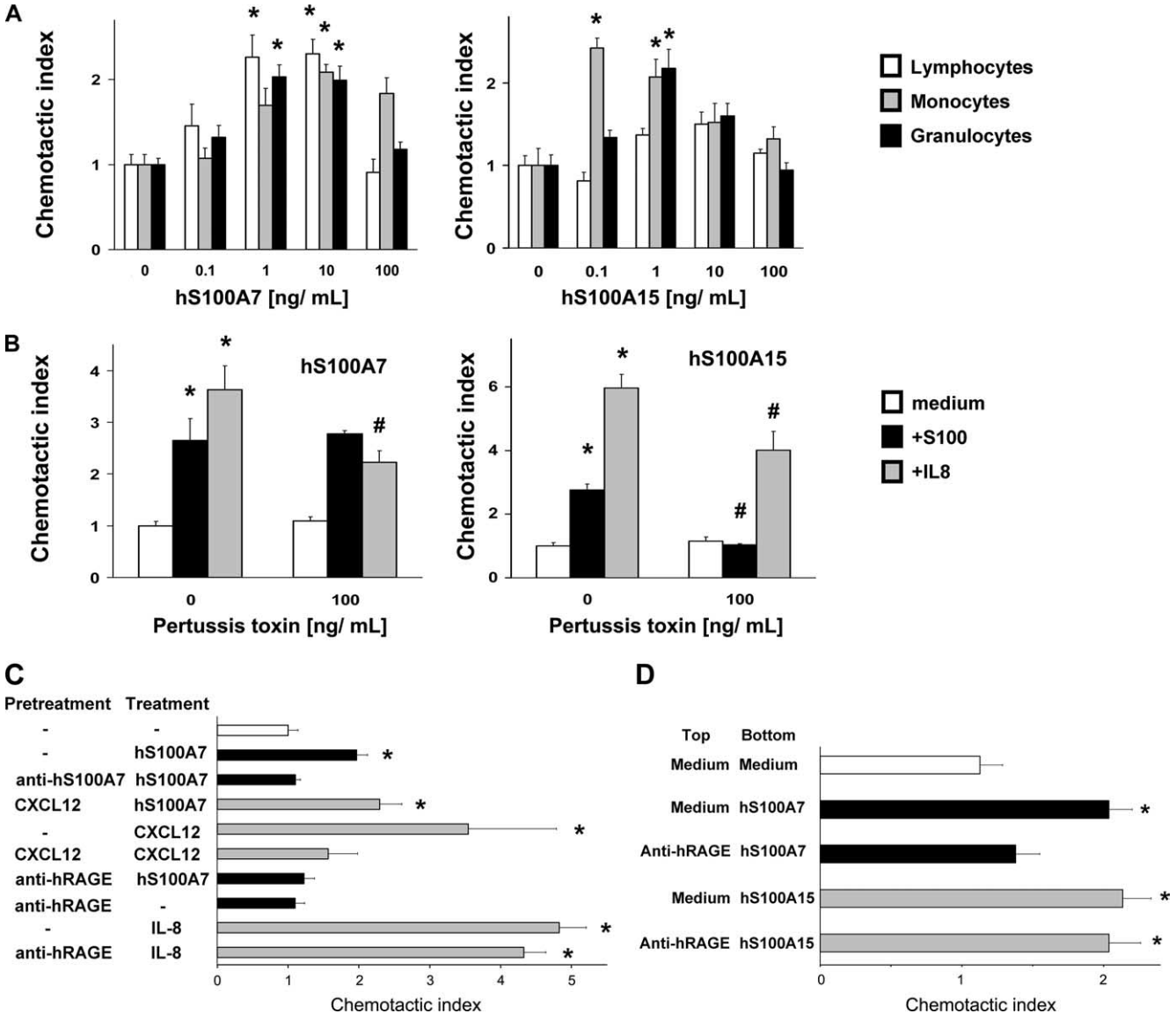

FIGURE 2. Both hS100A7 and hS100A15 are chemoattractants in vitro, but they differ in cell targets and receptor activation. *A*, Chemotactic response of indicated leukocyte subsets from peripheral blood of human volunteers, evaluated using micro-Boyden chambers of specific pore size. Migrating cells on the filter surface of the lower chamber were stained for counting (1 ng/ml = 88.5 nM S100 protein). *B–D*, Chemotactic response of granulocytes (*B*) with/without pertussis toxin pretreatment; (*C*) pretreated (pretreatment) with medium, anti-hS100A7, CXCL12, anti-hRAGE before incubation (treatment) with medium, hS100A7, CXCL12, and CXCL8/IL-8 as indicated; and (*D*) with mediators placed in the top (medium, anti-hRAGE) or bottom (medium, hS100A7, hS100A15) chambers. ∗, Chemotactic index ≥2 of six samples from at least three individual volunteers; #, statistically different compared with corresponding treatments ($p \leq 0.05$). Each bar represents mean, error bars indicate SD.

suprabasal compartments. Additionally, hS100A15 is highly expressed by basal psoriatic keratinocytes at the epidermal-stroma junction, as well as by dendritic and stromal cells in the dermis. Their differential expression in multiple cell types in different compartments of the skin might reflect their divergence and functional synergism, with implications for disease pathogenesis.

Both hS100A7 and hS100A15 are chemoattractants in vitro, but differ in cell targets and receptor activation

Both human S100A7 and S100A15 were identified in psoriasis and up-regulated in psoriasis, suggesting involvement in the inflammatory phenotype (1, 6). To investigate the possibility that these proteins attracted some of the inflammatory cells, we analyzed the chemotactic ability of hS100A7 and hS100A15 in a dual chamber assay (Fig. 2*A*). hS100A15 was identified as chemotactic for both granulocytes and monocytes, but not for lymphocytes. In contrast, hS100A7 attracted all three leukocyte populations at similar concentrations. In both cases, chemotaxis diminished at 100 ng/ml, developing an overall bell-shaped response that is typical for chemokines (18). To examine the role for a Gi protein-coupled receptor (GiPCR) in the chemotactic response, the assay was performed in the presence of pertussis toxin (Fig. 2*B*). hS100A15-mediated chemotaxis was attenuated upon pertussis toxin treatment, indicating signaling through a GiPCR. In contrast, pertussis toxin did not affect the hS100A7-induced neutrophil migration. As a positive control for the assay, IL-8 chemotaxis, mediated by the GiPCR CXCR1/2, was reduced by the pertussis toxin treatment.

A series of additional studies were performed to further elucidate the nature of the chemotactic receptors (Fig. 2*C*). hS100A7-mediated chemotaxis could be inhibited by the specific anti-hS100A7 Ab but could not be desensitized through activation of the classical pertussis toxin-sensitive interaction of CXCL12 with

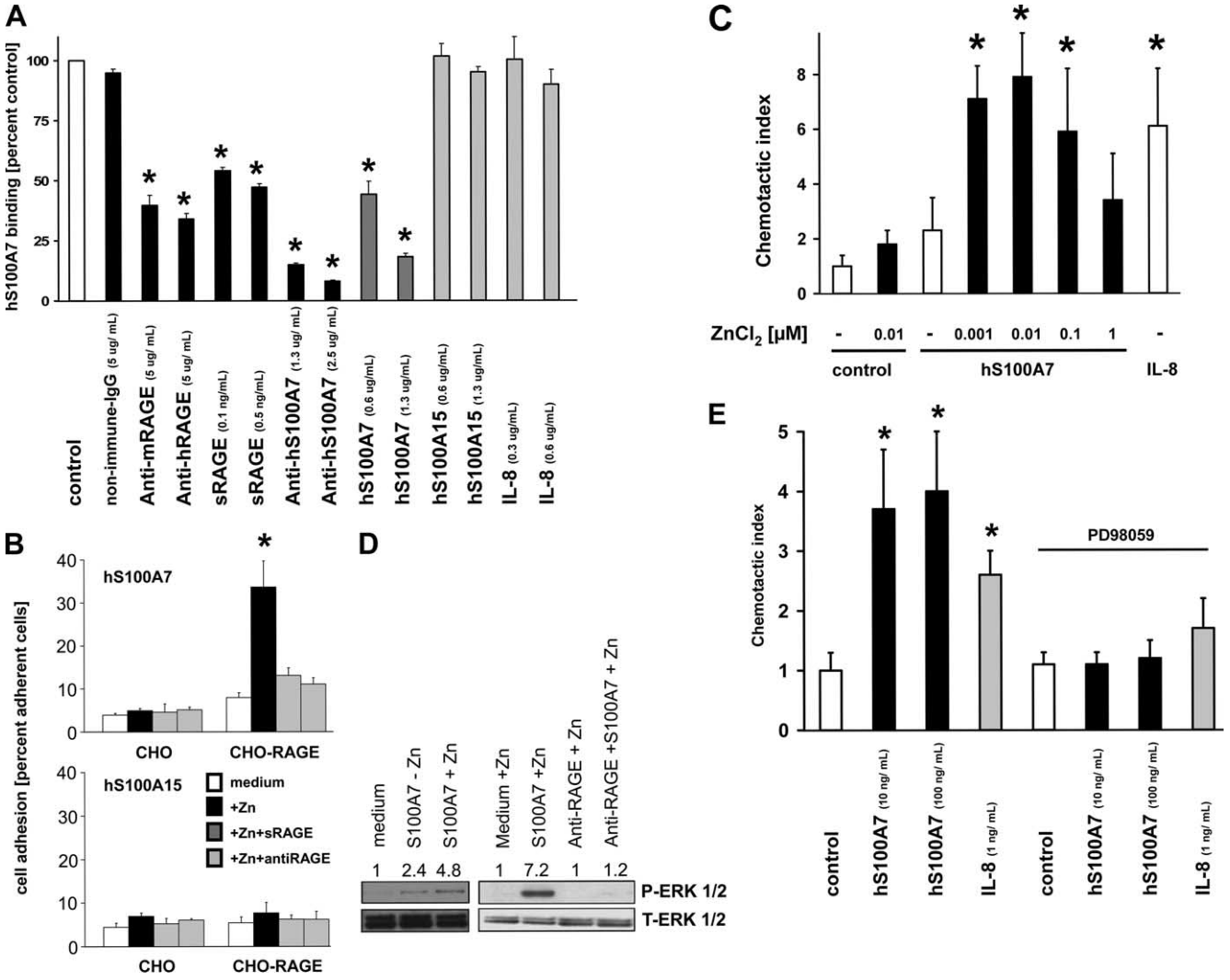

FIGURE 3. Binding, signaling, and chemotaxis of hS100A7 is dependent on RAGE binding and zinc in vitro. *A*, Competitive ligand binding assay employing 200 ng of biotinylated hS100A7 binding to 100 ng murine soluble RAGE coated on polystyrene plates. Unlabeled competitors were added for 90 min at indicated concentrations and followed by streptavidin-alkaline phosphatase. Readout was performed as a luminescence signal (representative of two separate experiments, $n = 3$; $*$, $p \leq 0.05$). *B*, Cell adhesion assay employing control or murine RAGE-transfected CHO cells to adhere to human S100A7 or human S100A15 in the absence and presence of zinc. Shaded bars show adhesion in the presence of soluble RAGE or anti-RAGE (representative of three independent experiments, $n = 3$; $*$, $p \leq 0.05$). *C*, Chemotactic response of human peripheral granulocytes toward hS100A7 in the lower chamber in the absence or presence of increasing concentrations of zinc (representative of three independent experiments, $n = 6$; $*$, $p \leq 0.05$). *D*, MAP kinase activation was determined in human peripheral blood neutrophils exposed to hS100A7 with/without zinc chloride (15 nM). In some cases, cells were pretreated with RAGE-neutralizing Abs. Cell lysates were gel-separated and subjected to immunoblotting with indicated Abs. Numbers above the lanes indicate relative phospho-ERK/total ERK increase. *E*, Chemotaxis of human peripheral blood neutrophils exposed to hS100A7 or IL-8/CXCL8 and pretreated with ERK inhibitor PD98059 (10 μM) in the lower well of Boyden chambers. Migrating cells on the filter of lower chamber side were stained and counted ($n = 6$; $*$, chemotactic index ≥ 2). Each bar represents mean of six samples from at least three individual volunteers, error bars indicate SD.

CXCR4. In contrast, blocking of RAGE by neutralizing Abs abolished the hS100A7-mediated chemotaxis, but not the IL-8-mediated effect. To confirm a role of RAGE in hS100A7-mediated chemotaxis, hS100A7 was placed in the bottom chamber and normal RAGE-bearing granulocytes were added to the upper chamber (Fig. 2*D*). When neutralizing anti-RAGE was added to the cells, hS100A7-mediated cell migration was inhibited, excluding undirected chemokinesis. In contrast, cell migration toward hS100A15 placed in the lower chamber was not affected by blocking RAGE on granulocytes in the upper chamber. Further, checkerboard analysis showed that hS100A7 and hS100A15 pro-migratory effects are mediated through chemotaxis (data not shown).

To address the nature of the pertussis toxin-sensitive hS100A15 receptor, desensitization experiments with ligands were performed that signal through GiPCR. Pretreatment of neutrophils with the ligands RANTES/CCL5, SDF-1/CXCL12, MCP-1/CCL2, and IL-8/CXCL8 did not attenuate the hS100A15-mediated chemotaxis, as opposed to corresponding ligand controls (data not shown). Due to the myeloid preference of hS100A15 and inability to attract mature or immature dendritic cells and lymphocytes, chemokine receptors that are preferentially expressed on lymphocytes or dendritic cells were excluded as potential targets for hS100A15 (CXCR 3, 5, and 6; CCR 4 and 6–10). BRAK/CXCL14 ligand (18, 19), which binds to an as yet unknown chemokine receptor(s), was able to desensitize hS100A15-mediated monocyte chemotaxis, whereas hS100A15 did not desensitize the chemotactic response to CXCL14 (data not shown). This unidirectional desensitization is probably based on the greater potency of CXCL14 than hS100A15.

To directly test the concept of hS100A7 and hS100A15 binding to different target receptors, ligand binding studies were performed

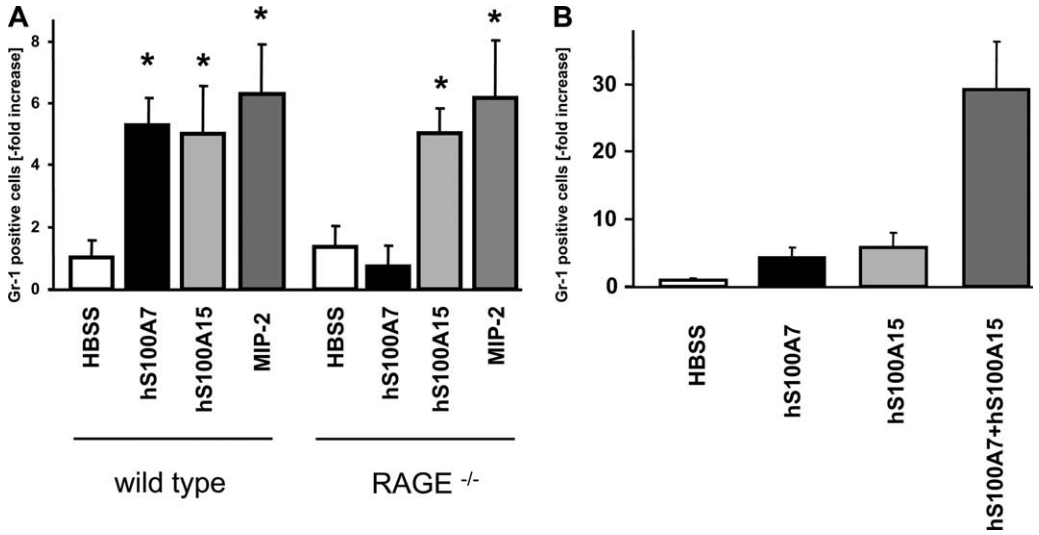

FIGURE 4. hS100A7 and hS100A15 act synergistically to induce inflamation in vivo, but they differ in receptor activation. Twenty micrograms of recombinant hS100A7, hS100A15, or MIP-2 were injected i.p. into C57BL/6 wild-type and RAGE$^{-/-}$ mice (*A*) alone or (*B*) premixed hS100A7 and hS100A15 (20 μg each) in combination. After 4 h, cells attracted into the peritoneal fluid were counted and analyzed by flow cytometry using the granulocyte marker Gr-1 (representative of three separate experiments, each time point represents the mean value + SD from six mice; *, $p \leq 0.05$).

(Fig. 3*A*). Biotinylated hS100A7 bound to immobilized purified RAGE, and binding could be blocked by increasing concentrations of unlabeled hS100A7. Biotinylated hS100A7 binding to RAGE substrate was inhibited in the presence of excess sRAGE, a truncated form of the receptor spanning the extracellular domain, and by anti-human and anti-mouse RAGE-IgG as well as anti-hS100A7. Unrelated casein or nonimmune IgG was without effect, as was competition with increasing concentrations of the hS100A15 paralog or IL-8.

Structural and biochemical data indicate that the S100A7 homodimer structure is altered through the binding and release of zinc, an important mediator in inflammation (20, 21). To test if zinc affects the hS100A7-RAGE interaction and function, hS100A7-mediated ligand binding, signaling, and chemotaxis were analyzed. Ligand binding experiments with RAGE in a natural cellular environment showed that adhesion of RAGE-transfected CHO cells to hS100A7-coated wells required zinc (Fig. 3*B*). The specificity of RAGE-hS100A7 interaction was shown by inhibition in the presence of excess sRAGE or neutralizing anti-RAGE IgG. Furthermore, the presence of zinc did not affect the lack of binding of RAGE-bearing cells toward plates coated with hS100A15. RAGE-deficient CHO cells transfected with a vector control did not adhere to plates coated with either S100 protein. Human neutrophils exposed to a gradient of recombinant hS100A7 protein in the absence of zinc showed no significant chemotactic response. The ability of hS100A7 to attract neutrophils was restored upon zinc replenishment (Fig. 3*C*). In line with zinc-dependent hS100A7-RAGE interaction and chemotaxis, neutrophils stimulated with hS100A7 showed RAGE-dependent phosphorylation of the migration-related MAPK ERK1/2 pathway (22) only in the presence of zinc (Fig. 3*D*). hS100A7-induced ERK1/2 phosphorylation was blocked by sRAGE (not shown) or neutralizing anti-RAGE IgG. The hS100A7-mediated chemotaxis was attenuated when neutrophils were pretreated with an ERK1/2 inhibitor, similar to IL-8 (Fig. 3*E*), indicating the requirement for ERK1/2 signaling for chemotactic response to hS100A7.

hS100A7 and hS100A15 are proinflammatory and synergistic in vivo but differ in receptor specificity

To test the concept that both hS100A7 and hS100A15 are chemoattractants in vivo, corresponding recombinant proteins were injected i.p. into C57BL/6 mice. Proinflammatory response was evaluated by analyzing cell count and cell type attracted into the peritoneal cavity. Both S100 proteins provoked an inflammatory response that was dose- and time-dependent and was absent when heat-inactivated S100 proteins were injected (data not shown). In C57BL/6 wild-type mice, a response was detected by 4 h for both proteins attracting Gr-1-positive cells compared with control (Fig. 4*A*). The hS100A7-induced inflammation was absent in RAGE$^{-/-}$ mice, whereas the hS100A15-mediated inflammatory response remained intact. As a positive control, i.p. injected MIP-2/mCXCL2 provoked an inflammation in both wild-type and RAGE$^{-/-}$ mice.

Since we found that hS100A7 and hS100A15 have distinct proinflammatory functions mediated through distinct mechanisms but are expressed in different compartments in the same inflammatory states, we tested for their combined effect as chemoattractants (Fig. 4*B*). Although i.p. application of either hS100A7 or hS100A15 provoked an inflammatory response (compare Fig. 4*A*), this was amplified substantially when both hS100A7 and hs100A15 were injected together. Thus, hS100A7 and hS100A15 act synergistically when co-expressed (Fig. 1*D*), suggesting that both proteins might contribute to the amplified inflammatory phenotype in psoriasis and other inflammatory diseases.

Discussion

Originally identified as a marker for psoriasis, hS100A7 (psoriasin) (1) and recently hS100A156 were found overexpressed in other inflammatory diseases (23–25). Physiologically, hS100A7 and hS100A15 may work together as part of an innate host defense controlling microbial growth on normal and inflamed skin (13, 26–28). Our current data indicate another function as chemoattractants for leukocytes. hS100A7 (13) and hS100A15 (25) are both regulated by proinflammatory cytokines that are predominant in inflammatory diseases, such as psoriasis (29, 30). That they are co-evolved, co-expressed, and co-regulated in identical pathological states begs the question of the biological significance of the evolutionary selection for these almost identical proteins.

Our data suggest a joint biological impact of hS100A7 and hS100A15 through evolutionary diversification. Both proteins are distinct in expression pattern, chemotactic activity, and functional mechanism. While each of them induces a proinflammatory response by itself, their proinflammatory activity is potentiated when

acting together, indicating that they contribute independently but synergistically to inflammation that may be fundamental to the disease phenotype. We provide mechanistic insights into hS100A7 and hS100A15 synergism by showing their biological diversity in expression in distinct cells in both normal and inflamed tissue, in receptor activation, and in chemotactic function. The documented up-regulation of hS100A7 in epithelial cancers (31) and similar findings for hS100A15 (data not shown) suggest that combined expression of these chemotactic proteins may contribute to other diseases as well. Having established specific Abs for each protein, we are now in a position to address this question. Furthermore, parallel targeting of hS100A7 and hS100A15 would allow a novel approach to treat associated diseases based on distinct mechanisms with possibly enhanced therapeutic efficacy (32, 33).

With the discovery of hS100A7 in 1991, structural and functional data have stimulated the quest for mechanistic clarification of its extracellular action (21, 34). The multiligand receptor RAGE is implicated in inflammatory processes, including leukocyte migration (12, 15, 35, 36). RAGE is expressed at low levels in normal tissues and becomes up-regulated wherever its ligands accumulate. Ligands initiate a sustained cellular activation through MAP kinases, culminating in the activation of NFκB (37, 38). Through recognition of β-sheet fibrillar structures or proinflammatory cytokine-like mediators of the S100/calgranulin family or high mobility group box-1 (HMGB-1), RAGE participates in the phenotype of inflammatory skin diseases, diabetes, amyloidosis, and promotes tumor progression (37, 39–43).

The identification of RAGE as a receptor for hS100A7 allows for specific targeting of hS100A7-mediated effects, such as cell migration in inflammation. Furthermore, with participation of RAGE in tumor growth and metastasis (43), hS100A7-RAGE interaction might be important to understand the role of secreted hS100A7 in epithelial tumorigenesis.

In contrast to hS100A7, hS100A15 preferentially attracts myeloid cells through a pertussis toxin-sensitive mechanism, suggesting signaling through a GiPCR. Two other chemotactic S100 proteins, S100-L and CP-10, bind to pertussis toxin-sensitive receptors, which, however, are yet to be identified (44, 45). Similar to CP-10, calcium mobilization through hS100A15 could not be detected (data not shown). This observation is consistent with the idea that S100 proteins are less potent than the classical chemoattractants. Homologous desensitization experiments with chemokine receptor ligands suggest that receptors preferentially active on myeloid cells (CXCR1/2, CCR1) or widespread receptors (CXCR4; CCR2, 3, and 5) are not involved in hS100A15-mediated chemotaxis. Collectively, our data suggest that hS100A15 binds to an unidentified GiPCR that also interacts with CXCL14.

hS100A15 is functionally active in the presence of calcium alone compared with hS100A7, suggesting that additional factors are important for hS100A7 chemotactic activity. Besides calcium, many S100 proteins bind zinc with high affinity, implying that divalent zinc is a major regulator of their extracellular function (13, 20, 21, 46). In hS100A7 (21) and others (37, 46, 47), the location of the zinc binding site is near one of the proposed target protein binding sites; however, mechanistic and functional consequences are undefined. We demonstrate that zinc is required for interaction and signaling of hS100A7 with the target protein RAGE and that it is functionally important for hS100A7-RAGE-mediated chemotaxis. Thus, our data indicate that zinc is a necessary co-factor for hS100A7-mediated proinflammatory activity. Together with previous studies (13, 26–28) showing that the antimicrobial action of hS100A7 was through zinc sequestration, we suggest that zinc may be involved in regulation of hS100A7 dual proinflammatory and antimicrobial functions.

For S100 proteins, individual physical and biochemical characteristics including the spatial structure of the S100 dimer/multimers determine the specificity of the target interaction (7, 48, 49). We have data suggesting that sequences and secondary structures of the hS100A7 and hS100A15 monomers are alike (6, 11). However, the quaternary structures of both proteins are distinct and could account for binding to different target receptors (B. Ahvazi et al., unpublished data). Furthermore, two of the amino acids divergent in hS100A7 and hS100A15 ($Thr^{52}Ile$, $Asn^{53}His$) appear to reside in a region that was shown to be a chemotactic domain for mouse S100A8 (50). If functionally conserved in hS100A7 and hS100A15, these differences might contribute as well to the distinct chemotactic properties of these highly homologous proteins.

Understanding the diversity and functional synergism of disease-associated proteins is crucial for developing therapeutic interventions based on distinct mechanisms with possibly enhanced therapeutic efficiency in S100A7- and S100A15-mediated pathological conditions. The unexpected different biology of almost identical proteins suggests that S100A7 and hS100A15 functional synergisms through biological diversification might underlie their biological impact, and thus their evolutionary selection.

Acknowledgments

We are grateful to Stephen Wincovitch and Susan Garfield for skillful assistance with confocal microscopy and Barbara Taylor for advice and help with the flow cytometry. We thank William Gillette and Jim Hartley for recombinant proteins, Roberta Smith for quantitative cell analysis, and Helen Rager for endotoxin analysis. We thank Christophe Cataisson for skillful help with the in vivo experiments and critical reading of the manuscript. We thank Alif Dharamsi for competent technical assistance, and Peter Nawroth and Angelika Bierhaus for providing $RAGE^{-/-}$ mice.

Disclosures

The authors have no financial conflicts of interest.

References

1. Madsen, P., H. H. Rasmussen, H. Leffers, B. Honore, K. Dejgaard, E. Olsen, J. Kiil, E. Walbum, A. H. Andersen, B. Basse, et al. 1991. Molecular cloning, occurrence, and expression of a novel partially secreted protein "psoriasin" that is highly up-regulated in psoriatic skin. *J. Invest. Dermatol.* 97: 701–712.
2. Boniface, K., F. X. Bernard, M. Garcia, A. L. Gurney, J. C. Lecron, and F. Morel. 2005. IL-22 inhibits epidermal differentiation and induces proinflammatory gene expression and migration of human keratinocytes. *J. Immunol.* 174: 3695–3702.
3. Boniface, K., C. Diveu, F. Morel, N. Pedretti, J. Froger, E. Ravon, M. Garcia, E. Venereau, L. Preisser, E. Guignouard, et al. 2007. Oncostatin M secreted by skin infiltrating T lymphocytes is a potent keratinocyte activator involved in skin inflammation. *J. Immunol.* 178: 4615–4622.
4. Eckert, R. L., A. M. Broome, M. Ruse, N. Robinson, D. Ryan, and K. Lee. 2004. S100 proteins in the epidermis. *J. Invest. Dermatol.* 123: 23–33.
5. Wolk, K., E. Witte, E. Wallace, W. D. Docke, S. Kunz, K. Asadullah, H. D. Volk, W. Sterry, and R. Sabat. 2006. IL-22 regulates the expression of genes responsible for antimicrobial defense, cellular differentiation, and mobility in keratinocytes: a potential role in psoriasis. *Eur. J. Immunol.* 36: 1309–1323.
6. Wolf, R., A. Mirmohammadsadegh, M. Walz, B. Lysa, U. Tartler, R. Remus, U. Hengge, G. Michel, and T. Ruzicka. 2003. Molecular cloning and characterization of alternatively spliced mRNA isoforms from psoriatic skin encoding a novel member of the S100 family. *FASEB J.* 17: 1969–1971.
7. Donato, R. 2003. Intracellular and extracellular roles of S100 proteins. *Microsc. Res. Tech.* 60: 540–551.
8. Heizmann, C. W., G. Fritz, and B. W. Schafer. 2002. S100 proteins: structure, functions and pathology. *Front. Biosci.* 7: d1356–d1368.
9. Kulski, J. K., C. P. Lim, D. S. Dunn, and M. Bellgard. 2003. Genomic and phylogenetic analysis of the S100A7 (psoriasin) gene duplications within the region of the S100 gene cluster on human chromosome 1q21. *J. Mol. Evol.* 56: 397–406.
10. Wolf, R., C. J. Voscopoulos, P. C. FitzGerald, P. Goldsmith, C. Cataisson, M. Gunsior, M. Walz, T. Ruzicka, and S. H. Yuspa. 2006. The mouse S100A15 ortholog parallels genomic organization, structure, gene expression, and protein-processing pattern of the human S100A7/A15 subfamily during epidermal maturation. *J. Invest. Dermatol.* 126: 1600–1608.
11. Boeshans, K. M., R. Wolf, C. Voscopoulos, W. Gillette, D. Esposito, T. C. Mueser, S. H. Yuspa, and B. Ahvazi. 2006. Purification, crystallization, and preliminary X-ray diffraction of human S100A15. *Acta Crystallogr. Sect. F Struct. Biol. Cryst. Commun.* 62: 467–470.
12. Orlova, V. V., E. Y. Choi, C. Xie, E. Chavakis, A. Bierhaus, E. Ihanus, C. M. Ballantyne, C. G. Gahmberg, M. E. Bianchi, P. P. Nawroth, and

T. Chavakis. 2007. A novel pathway of HMGB1-mediated inflammatory cell recruitment that requires Mac-1-integrin. *EMBO J.* 26: 1129–1139.
13. Glaser, R., J. Harder, H. Lange, J. Bartels, E. Christophers, and J. M. Schroder. 2005. Antimicrobial psoriasin (S100A7) protects human skin from *Escherichia coli* infection. *Nat. Immunol.* 6: 57–64.
14. Chertov, O., H. Ueda, L. L. Xu, K. Tani, W. J. Murphy, J. M. Wang, O. M. Howard, T. J. Sayers, and J. J. Oppenheim. 1997. Identification of human neutrophil-derived cathepsin G and azurocidin/CAP37 as chemoattractants for mononuclear cells and neutrophils. *J. Exp. Med.* 186: 739–747.
15. Chavakis, T., A. Bierhaus, N. Al Fakhri, D. Schneider, S. Witte, T. Linn, M. Nagashima, J. Morser, B. Arnold, K. T. Preissner, and P. P. Nawroth. 2003. The pattern recognition receptor (RAGE) is a counterreceptor for leukocyte integrins: a novel pathway for inflammatory cell recruitment. *J. Exp. Med.* 198: 1507–1515.
16. Foell, D., H. Wittkowski, T. Vogl, and J. Roth. 2007. S100 proteins expressed in phagocytes: a novel group of damage-associated molecular pattern molecules. *J. Leukocyte Biol.* 81: 28–37.
17. Harrison, C. A., M. J. Raftery, J. Walsh, P. Alewood, S. E. Iismaa, S. Thliveris, and C. L. Geczy. 1999. Oxidation regulates the inflammatory properties of the murine S100 protein S100A8. *J. Biol. Chem.* 274: 8561–8569.
18. Oppenheim, J. J., D. Yang, A. Biragyn, O. M. Howard, and P. Plotz. 2002. Chemokine receptors on dendritic cells promote autoimmune reactions. *Arthritis Res.* 4 (*Suppl.* 3): S183–S188.
19. Hromas, R., H. E. Broxmeyer, C. Kim, H. Nakshatri, K. Christopherson, M. Azam, and Y. H. Hou. 1999. Cloning of BRAK, a novel divergent CXC chemokine preferentially expressed in normal versus malignant cells. *Biochem. Biophys. Res. Commun.* 255: 703–706.
20. Vorum, H., P. Madsen, H. H. Rasmussen, M. Etzerodt, I. Svendsen, J. E. Celis, and B. Honore. 1996. Expression and divalent cation binding properties of the novel chemotactic inflammatory protein psoriasin. *Electrophoresis* 17: 1787–1796.
21. Brodersen, D. E., J. Nyborg, and M. Kjeldgaard. 1999. Zinc-binding site of an S100 protein revealed: two crystal structures of Ca^{2+}-bound human psoriasin (S100A7) in the Zn^{2+}-loaded and Zn^{2+}-free states. *Biochemistry* 38: 1695–1704.
22. Nakamae-Akahori, M., T. Kato, S. Masuda, E. Sakamoto, H. Kutsuna, F. Hato, Y. Nishizawa, M. Hino, and S. Kitagawa. 2006. Enhanced neutrophil motility by granulocyte colony-stimulating factor: the role of extracellular signal-regulated kinase and phosphatidylinositol 3-kinase. *Immunology* 119: 393–403.
23. Algermissen, B., J. Sitzmann, P. LeMotte, and B. Czarnetzki. 1996. Differential expression of CRABP II, psoriasin, and cytokeratin 1 mRNA in human skin diseases. *Arch. Dermatol. Res.* 288: 426–430.
24. Di Nuzzo, S., R. M. Sylva-Steenland, C. W. Koomen, M. A. de Rie, P. K. Das, J. D. Bos, and M. B. Teunissen. 2000. Exposure to UVB induces accumulation of LFA-1^+ T cells and enhanced expression of the chemokine psoriasin in normal human skin. *Photochem. Photobiol.* 72: 374–382.
25. Wolf, R., V. Lewerenz, A. S. Buchau, M. Walz, and T. Ruzicka. 2007. Human S100A15 splice variants are differentially expressed in inflammatory skin diseases and regulated through Th1 cytokines and calcium. *Exp. Dermatol.* 16: 685–691.
26. Buchau, A. S., M. Hassan, G. Kukova, V. Lewerenz, S. Kellermann, J. U. Wurthner, R. Wolf, M. Walz, R. L. Gallo, and T. Ruzicka. 2007. S100A15, an antimicrobial protein of the skin: regulation by *E. coli* through Toll-like receptor 4. *J. Invest. Dermatol.* 127: 2596–2604.
27. Lee, K. C., and R. L. Eckert. 2007. S100A7 (psoriasin): mechanism of antibacterial action in wounds. *J. Invest. Dermatol.* 127: 945–957.
28. Schroder, J. M., and J. Harder. 2006. Antimicrobial skin peptides and proteins. *Cell Mol. Life Sci.* 63: 469–486.
29. Griffiths, C. E. 2003. The immunological basis of psoriasis. *J. Eur. Acad. Dermatol. Venereol.* 17 (*Suppl.* 2): 1–5.
30. Lew, W., A. M. Bowcock, and J. G. Krueger. 2004. *Psoriasis vulgaris*: cutaneous lymphoid tissue supports T-cell activation and "type 1" inflammatory gene expression. *Trends Immunol.* 25: 295–305.
31. Al Haddad, S., Z. Zhang, E. Leygue, L. Snell, A. Huang, Y. Niu, T. Hiller-Hitchcock, K. Hole, L. C. Murphy, and P. H. Watson. 1999. Psoriasin (S100A7) expression and invasive breast cancer. *Am. J. Pathol.* 155: 2057–2066.
32. Daly, C., and B. J. Rollins. 2003. Monocyte chemoattractant protein-1 (CCL2) in inflammatory disease and adaptive immunity: therapeutic opportunities and controversies. *Microcirculation* 10: 247–257.
33. Luster, A. D., R. Alon, and U. H.von Andrian. 2005. Immune cell migration in inflammation: present and future therapeutic targets. *Nat. Immunol.* 6: 1182–1190.
34. Jinquan, T., H. Vorum, C. G. Larsen, P. Madsen, H. H. Rasmussen, B. Gesser, M. Etzerodt, B. Honore, J. E. Celis, and K. Thestrup-Pedersen. 1996. Psoriasin: a novel chemotactic protein. *J. Invest. Dermatol.* 107: 5–10.
35. Bierhaus, A., P. M. Humpert, M. Morcos, T. Wendt, T. Chavakis, B. Arnold, D. M. Stern, and P. P. Nawroth. 2005. Understanding RAGE, the receptor for advanced glycation end products. *J. Mol. Med.* 83: 876–886.
36. Schmidt, A. M., S. D. Yan, S. F. Yan, and D. M. Stern. 2001. The multiligand receptor RAGE as a progression factor amplifying immune and inflammatory responses. *J. Clin. Invest.* 108: 949–955.
37. Hofmann, M. A., S. Drury, C. Fu, W. Qu, A. Taguchi, Y. Lu, C. Avila, N. Kambham, A. Bierhaus, P. Nawroth, et al. 1999. RAGE mediates a novel proinflammatory axis: a central cell surface receptor for S100/calgranulin polypeptides. *Cell* 97: 889–901.
38. Sorci, G., F. Riuzzi, A. L. Agneletti, C. Marchetti, and R.Donato. 2003. S100B inhibits myogenic differentiation and myotube formation in a RAGE-independent manner. *Mol. Cell. Biol.* 23: 4870–4881.
39. Deane, R., Y. S. Du, R. K. Submamaryan, B. LaRue, S. Jovanovic, E. Hogg, D. Welch, L. Manness, C. Lin, J. Yu, et al. 2003. RAGE mediates amyloid-β peptide transport across the blood-brain barrier and accumulation in brain. *Nat. Med.* 9: 907–913.
40. Dumitriu, I. E., P. Baruah, A. A. Manfredi, M. E. Bianchi, and P. Rovere-Querini. 2005. HMGB1: guiding immunity from within. *Trends Immunol.* 26: 381–387.
41. Lotze, M. T., and K. J. Tracey. 2005. High-mobility group box 1 protein (HMGB1): nuclear weapon in the immune arsenal. *Nat. Rev. Immunol.* 5: 331–342.
42. Park, L., K. G. Raman, K. J. Lee, Y. Lu, L. J. Ferran, Jr., W. S. Chow, D. Stern, and A. M. Schmidt. 1998. Suppression of accelerated diabetic atherosclerosis by the soluble receptor for advanced glycation endproducts. *Nat. Med.* 4: 1025–1031.
43. Taguchi, A., D. C. Blood, G. del Toro, A. Canet, D. C. Lee, W. Qu, N. Tanji, Y. Lu, E. Lalla, C. Fu, et al. 2000. Blockade of RAGE-amphoterin signalling suppresses tumour growth and metastases. *Nature* 405: 354–360.
44. Cornish, C. J., J. M. Devery, P. Poronnik, M. Lackmann, D. I. Cook, and C. L. Geczy. 1996. S100 protein CP-10 stimulates myeloid cell chemotaxis without activation. *J. Cell. Physiol.* 166: 427–437.
45. Komada, T., R. Araki, K. Nakatani, I. Yada, M. Naka, and T. Tanaka. 1996. Novel specific chemotactic receptor for S100L protein on guinea pig eosinophils. *Biochem. Biophys. Res. Commun.* 220: 871–874.
46. Miranda, L. P., T. Tao, A. Jones, I. Chernushevich, K. G. Standing, C. L. Geczy, and P. F. Alewood. 2001. Total chemical synthesis and chemotactic activity of human S100A12 (EN-RAGE). *FEBS Lett.* 488: 85–90.
47. Xie, J., D. S. Burz, W. He, I. B. Bronstein, I. Lednev, and A. Shekhtman. 2007. Hexameric calgranulin C (S100A12) binds to the receptor for advanced glycated end products (RAGE) using symmetric hydrophobic target-binding patches. *J. Biol. Chem.* 282: 4218–4231.
48. Santamaria-Kisiel, L., A. C. Rintala-Dempsey, and G. S. Shaw. 2006. Calcium-dependent and -independent interactions of the S100 protein family. *Biochem. J.* 396: 201–214.
49. Zimmer, D. B., S. P. Wright, and D. J. Weber. 2003. Molecular mechanisms of S100-target protein interactions. *Microsc. Res. Tech.* 60: 552–559.
50. Ravasi, T., K. Hsu, J. Goyette, K. Schroder, Z. Yang, F. Rahimi, L. P. Miranda, P. F. Alewood, D. A. Hume, and C. Geczy. 2004. Probing the S100 protein family through genomic and functional analysis. *Genomics* 84: 10–22.